Tunable Terahertz-Wave Parametric Oscillators Using $LiNbO_3$ and $MgO:LiNbO_3$ Crystals

Jun-ichi Shikata, Kodo Kawase, Ken-ichi Karino, Tetsuo Taniuchi, and Hiromasa Ito, *Senior Member, IEEE*

***Abstract*—Coherent tunable terahertz waves were generated successfully using a terahertz-wave parametric oscillator (TPO) based on laser light scattering from the A_1-symmetry polariton mode of $LiNbO_3$. This method has several advantages, such as continuous and wide tunability (frequency: 0.9–3.1 THz), a relatively high peak power (more than a few milliwatts), and compactness of its system (tabletop size). In addition, the system simply requires a fixed-wavelength pump source, and it is easy to tune. This paper deals with the general performance of this terahertz-wave source using the prism output-coupler method as well as the development and applications of the system. Its tunability, coherency, power, and polarization were measured, and this tunable source was used for terahertz spectroscopy to measure the absorption spectra of $LiNbO_3$ and water vapor. Also, the use of MgO-doped $LiNbO_3$ ($MgO:LiNbO_3$) in our terahertz regime, as well as its far-infrared properties, is described. We found that the $MgO:LiNbO_3$ TPO is almost five times more efficient than the undoped $LiNbO_3$ TPO, and we have proven that the enhancement mechanism originates from the enhanced scattering cross section of the lowest A_1-symmetry mode in a spontaneous Raman experiment.**

***Index Terms*—MgO-doped $LiNbO_3$, nonlinear, parametric, spectroscopy, terahertz, tunable.**

I. Introduction

TRADITIONALLY, experimental science and technology in the terahertz-wave region of electromagnetic spectrum have lagged behind developments in the microwave region and the infrared and optical regions. Therefore, it is highly likely that new phenomena will be found in this frequency range in the basic and applied physics, the life science, the communication, and so forth. Over the past few years, compact and easy-handling terahertz-wave sources using the recent laser technology have attracted much attention from both fundamental and applied perspectives. Mainly, these research efforts are classified into the following two categories. One is the ultrashort-pulse terahertz-wave generation using high-speed photoconductive (PC) antennas, semiconductor, or superconductor materials pumped with a mode-locked femtosecond laser [1]–[8]. Typically, the spectral density spans from below 100 GHz to more than a few terahertz, reflecting the Fourier transform of the short laser pulse and the response of the irradiated material. With the advent of the terahertz time-domain spectroscopy [1]–[8], signal-to-noise ratio is much improved than that of conventional far-infrared Fourier-transform spectrometers using low-brightness incoherent sources and bolometric detectors. The other research current is on the coherent tunable terahertz-wave generation based on the nonlinear frequency conversion of the (quasi-)continuous-wave laser light [9]–[22]. The terahertz radiation has a sharp spectral characteristic and continuous tunability (typically, in the frequency range from subterahertz to more than a few terahertz). Therefore, the terahertz-wave source is expected to be useful for wide ranges of applications, such as spectroscopic studies without a monochromator, coherent excitation of materials, wavelength-dependent imaging, local oscillators, and so forth. This terahertz-wave generation method includes the difference-frequency mixing between two laser sources on nonlinear optical materials [9], [10] or PC antennas [11], [12], and the laser-pumped parametric oscillation using both second- and third-order nonlinearities [13]–[22]. While the difference-frequency method requires at least one tunable laser source, the parametric method simply requires a fixed-wavelength laser source. In addition, the latter method has achieved more than several-order higher conversion efficiency than the former method.

For the efficient generation of a terahertz wave using the parametric method, $LiNbO_3$ is one of the most suitable materials because of its large nonlinear coefficient [23], [24] and its wide transparency range [23], [25]. However, a large refractive index and a large absorption coefficient at terahertz frequencies [25], [26] are problems because efficiently generated terahertz waves suffer total reflections and large absorption losses. We have developed a tunable terahertz-wave parametric oscillator (TPO) that operates at room temperature using $LiNbO_3$ with new output coupling methods for the terahertz wave (grating-coupler method [15], [16], Si-prism-coupler method [17]–[22]) to substantially improve its efficiency. A tunability from 0.9 to 3.1 THz and the peak power of more than a few milliwatts was achieved using a nanosecond pump laser [15]–[22]. Furthermore, we recently increased the terahertz-wave output more than 100 times by cooling the crystal, which enhanced parametric gain and reduced the absorption loss at terahertz frequency [21], [22]. A linearly polarized terahertz-wave beam is emitted from the TPO with the divergence of less than a few degrees, and its beam profile has a Gaussian-like characteristic [15]–[22].

In this paper, we show the performance and application of this terahertz-wave source. We also describe the recent

Manuscript received March 1, 1999; revised September 10, 1999. This work was supported in part by the Ministry of Education, Science, and Culture of Japan under a Grant-in-Aid, and by the Research Foundation for Opto-Science and Technology under a grant.

J. Shikata, K. Karino, and T. Taniuchi are with the Research Institute of Electrical Communication, Tohoku University, Sendai 980-8577, Japan (e-mail: shikata@riec.tohoku.ac.jp).

K. Kawase is with the Photo Dynamics Research Center, RIKEN, Sendai 980-0608, Japan.

H. Ito is with the Research Institute of Electrical Communication, Tohoku University, Sendai 980-8577, Japan, and is also with the Photo Dynamics Research Center, RIKEN, Sendai 980-0608, Japan.

Publisher Item Identifier S 0018-9480(00)02534-5.

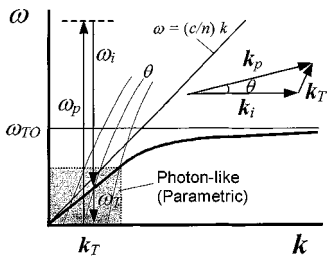

Fig. 1. Dispersion relation of the polariton, an elementary excitation generated by the combination of a photon and a TO phonon ($\omega_{\rm TO}$). The polariton in the low-energy region behaves like a photon at terahertz frequency. Due to the phase-matching condition, as well as the energy conservation law, which hold in the stimulated parametric process, a tunable terahertz wave is obtained by the control of the wave vector $\boldsymbol{k}_T$. The inset shows the noncollinear phase-matching condition.

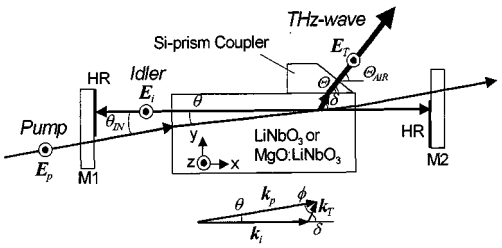

Fig. 2. Experimental cavity arrangement for the terahertz-wave generation using an Si-prism coupler on the y-surface of the $LiNbO_3$ crystal. The inset shows the noncollinear phase-matching condition.

works on the MgO-doped $LiNbO_3$ ($MgO:LiNbO_3$) TPO to achieve higher terahertz-wave output and wider tunability. The $MgO:LiNbO_3$ crystal has remarkably stronger resistance to the optical damage than undoped one [27], and nonlinear d-coefficients slightly increase with the dope [24]. Highly efficient nonlinear frequency conversion was also reported in the visible and near infrared region [28], [29]; however, as far as we know, an $MgO:LiNbO_3$ parametric oscillator at terahertz frequency has not been studied. We demonstrate the advanced performance of the TPO, as well as the far-infrared properties of the crystal studied by parametric generation, Raman spectroscopy, and far-infrared transmittance.

II. Principle of Operation

A. Tunable Terahertz-Wave Generation Using Polariton

The generation of coherent tunable terahertz-waves results from the efficient parametric scattering of laser light via polariton (stimulated polariton scattering [30]–[32]). Polariton is a quanta of the coupled phonon–photon transverse-wave field, and the stimulated polariton scattering occurs in polar crystals, such as $LiNbO_3$, $LiTaO_3$ and GaP, which are both infrared and Raman active, when pump excitation is sufficiently strong [30]–[32]. The scattering process involves both second- and third-order nonlinear processes [30]–[32], thus, the strong interaction occurs among the pump, the idler, and the polariton (terahertz) waves. For generating terahertz waves efficiently, $LiNbO_3$ is one of the most suitable materials because of its large nonlinear coefficient ($d_{33} = 25.2$ pm/V @ $\lambda = 1.064$ μm [24]) and its transparent characteristics in a wide-wavelength range (0.4–5.5 μm [23], [25]). $LiNbO_3$ has four infrared- and Raman-active transverse optical (TO) phonon modes called A_1-symmetry modes, and the lowest mode ($\omega_0 \sim 250$ cm^{-1}) is useful for efficient tunable far-infrared generation because of the largest parametric gain, as well as the smallest absorption coefficient [13], [14], [32].

The principle of the tunable TPO is as follows. Polaritons exhibit phonon-like behavior in the resonant frequency region (near the TO-phonon frequency ω_{TO}). However, they behave like photons in the nonresonant low-frequency region (Fig. 1), where a signal photon at terahertz frequency (ω_T) and a near-infrared idler photon (ω_i) are created parametrically from a near-infrared pump photon (ω_p), according to the energy conservation law $\omega_p = \omega_T + \omega_i$ (p: pump, T: terahertz, i: idler). In the stimulated scattering process, the momentum conservation law $\boldsymbol{k}_p = \boldsymbol{k}_T + \boldsymbol{k}_i$ (noncollinear phase-matching condition; see the insets of Figs. 1 and 2) also holds. This leads to the angle-dispersive characteristics of the idler and terahertz waves generated. Thus, a coherent terahertz wave is generated efficiently by using the optical resonator for the idler wave, as shown in Fig. 2, and the continuous and wide tunability is accomplished simply by changing the angle $\theta_{\rm IN}$ between the incident pump beam and the resonator axis (angle-tuning).

B. Theory of Parametric Gain

In the stimulated polariton scattering, the four fields, namely the pump $\boldsymbol{E}_p$, the idler $\boldsymbol{E}_i$, the terahertz wave $\boldsymbol{E}_T$, and the ionic vibration $\boldsymbol{Q}_0$ (lowest A_1 mode), mutually interact. The parametric gain coefficients for the idler and terahertz waves are obtained by solving the classical coupled-wave equations that describe this phenomenon. Assuming a steady state and no pump depletion, the coupled-wave equations are written as [30]–[32]

$$\left[\nabla^2 + \frac{\omega^2}{c^2}\varepsilon_T\right] E_T = -\frac{\omega^2}{c^2}\chi_P E_p E_i^*$$
$$\left[\nabla^2 + \frac{\omega_i^2}{c^2}\left(\varepsilon_i + \chi_R |E_p|^2\right)\right] E_i = -\frac{\omega_i^2}{c^2}\chi_P E_p E_T^* \qquad (1)$$

where $\omega_i (= \omega_p - \omega)$ denote frequencies of the idler, ω denote frequencies of the terahertz wave, $\varepsilon_\beta (\beta = T, i)$ is the permittivity in the material ($LiNbO_3$), and c is the velocity of light in a vacuum. The nonlinear susceptibilities χ_P and χ_R denote parametric and Raman processes, respectively, and they are expressed as [32]

$$\chi_P = d_E + \frac{S_0\omega_0^2}{\omega_0^2 - \omega^2}\cdot d_Q \qquad (2)$$

$$\chi_R = \frac{S_0\omega_0^2}{\omega_0^2 - \omega^2 - i\omega\Gamma_0}\cdot d_Q^2 \qquad (3)$$

where ω_0, S_0, and Γ_0 are the eigenfrequency, oscillator strength, and damping coefficient (or linewidth) of the lowest A_1-symmetry phonon mode, respectively. Coefficients $d_E (= 16\pi d_{33})$ and d_Q denote the second- and third-order nonlinear processes, which originate from electronic and ionic polarization, respectively. According to the rate equation analysis, the expression of d_Q in cgs units is given by [32]

$$d_Q = \left[\frac{8\pi c^4 n_p (S_{33}/L\Delta\Omega)_0}{S_0\hbar\omega_0\omega_i^4 n_i(\overline{n}_0 + 1)}\right]^{1/2} \qquad (4)$$

where $n_\beta(\beta = p, i)$ is the refractive index and $\overline{n}_0 = (\exp[\hbar\omega_0/\mathrm{kT}] - 1)^{-1}$ ($\hbar$: Planck constant, k: Boltzman constant, T: temperature) is the Bose distribution function. The quantity $(S_{33}/L\Delta\Omega)_0$ denotes the spontaneous-Raman (Stokes) scattering efficiency of the lowest A_1-symmetry phonon mode, where S_{33} is the fraction of incident power that is scattered into a solid angle $\Delta\Omega$ near a normal to the optical path length L [33], and it is proportional to the scattering cross section.

The coupled wave equations (1) can be solved using the plane-wave approach, and analytical expressions of the exponential gain for the terahertz wave and idler are [32]

$$g_T = g_i \cos\phi = \frac{\alpha_T}{2}\left\{\left[1 + 16\cos\phi\left(\frac{g_0}{\alpha_T}\right)^2\right]^{1/2} - 1\right\} \tag{5}$$

where ϕ is the phase-matching angle between the pump and the terahertz wave, g_0 is the low-loss limit, and α_T is an absorption coefficient in the terahertz region. In cgs units, they are written as [32]

$$g_0 = \left(\frac{\pi\omega\omega_i I_p}{2c^3 n_T n_i n_p}\right)^{1/2}\chi_P \tag{6}$$

$$\alpha_T = 2|\mathrm{Im}\, k_T| = \frac{2\omega}{c}\mathrm{Im}\left[\varepsilon_\infty + \frac{S_0\omega_0^2}{\omega_0^2 - \omega^2 - i\omega\Gamma_0}\right]^{1/2}. \tag{7}$$

The low-loss parametric gain g_0 has the same form as the parametric gain in the optical region [34], but the nonlinear susceptibility χ_P, which involve both second- and third-order processes (2), is almost determined by the third-order (ionic) d_Q-term (over 80% contribution).

Physical meaning of the susceptibility χ_P is explained as follows [31]. According to the simple classical picture, polar crystal such as $LiNbO_3$ is considered to be an ensemble of individual molecular systems, where the molecule consists of nuclei bonded together and surrounded by an electron cloud. When the crystal is irradiated by the pump laser polarized along the z-axis of the crystal, the relatively light electron cloud absorbs the pump energy and follows the incident field, and the electronic dipole moment appears due to the displacement of the electron charge cloud with respect to the nuclei. This is the origin of the second-order nonlinearity expressed by the d_E (or d_{33}) coefficient. Next, some of the energy absorbed by the electrons is transferred to the nuclei and two nuclei begin to vibrate (i.e., phonons are created) because the A_1-symmetry modes are infrared active. This phenomenon leads to the ionic dipole moment or the third-order nonlinearity expressed by the Raman susceptibility χ_R (Stokes process). Finally, the ionic vibration modulates the electronic vibration, and the electron–ion interaction occurs because the vibrations are along the z-axis. Thus, the three-photon parametric scattering process among the pump, the Stokes (idler) and the terahertz (polariton) waves involves both second- and third-order nonlinearities.

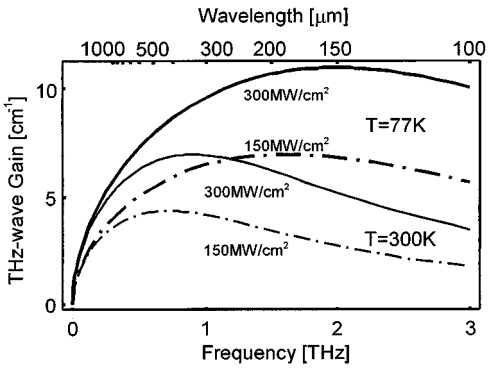

Fig. 3. Calculated gain coefficient for the parametric terahertz-wave generation using $LiNbO_3$ crystal pumped at 1.064 μm. The gain is enhanced by cooling the crystal due to the reduced absorption loss at terahertz frequency.

Fig. 3 shows the calculated parametric gain g_T for $LiNbO_3$ at typical pump intensities. A gain in the order of several cm^{-1} is feasible in the frequency domain up to 3 THz at room temperature, and the gain is enhanced by cooling the crystal [21], [22]. The decrease in the linewidth Γ_0 of the lowest A_1-symmetry phonon mode [33] makes the major contribution to the enhancement at low temperature because a_T is nearly in proportion to Γ_0 (7). The reduced linewidth reduces the absorption coefficient α_T at terahertz frequency, enhancing the parametric gain g_T, which is a monotonically decreasing function of the absorption coefficient (5). Physically, when the polariton damping caused by random thermal activation is reduced and the polariton has longer life time, the parametric interaction efficiently occurs. It is also possible to increase the parametric gain by increasing the pump intensity or by using a shorter wavelength pump source because the gain is a monotonically increasing function of g_0, which is proportional to $[(\omega_p - \omega_T)\cdot I_p]^{1/2}$.

C. TPO Using the Prism Output-Coupler Method

In the previous section, the parametric amplification process via polariton in the single-pass configuration was described. In order to produce oscillation, feedback at the idler wavelength ($\sim$1.07 μm for a $\sim$1.064-μm pump wavelength) is necessary (Fig. 2). Although the three waves (pump, idler, and terahertz wave) interact efficiently in the parametric oscillation, most of the terahertz wave generated is absorbed or totally reflected inside the $LiNbO_3$ crystal. This is due to the heavy absorption loss [more than several tens cm^{-1} and the large refractive index ($>$5) in the terahertz range [25]. To overcome the problem, we have proposed the TPO configuration using the prism coupler [17]–[22], as shown in Fig. 2.

Since the refractive index of Si is almost fixed to be 3.4 and its absorption coefficient is relatively small ($\sim$0.6 cm^{-1}) in the terahertz region [26], the terahertz wave generated inside $LiNbO_3$ is efficiently coupled out via an Si-prism according to Snell's law. In addition, the radiation angle Θ inside the prism is almost constant due to the ultra-low dispersion characteristics of Si in the terahertz region, though the phase-matching angle δ changes inside the crystal by rotating the cavity stage. Therefore, the direction Θ_{AIR} of the terahertz wave outside the prism is almost fixed for the entire tuning range ($\sim$0.5° for wavelengths from 150 to 300 μm).

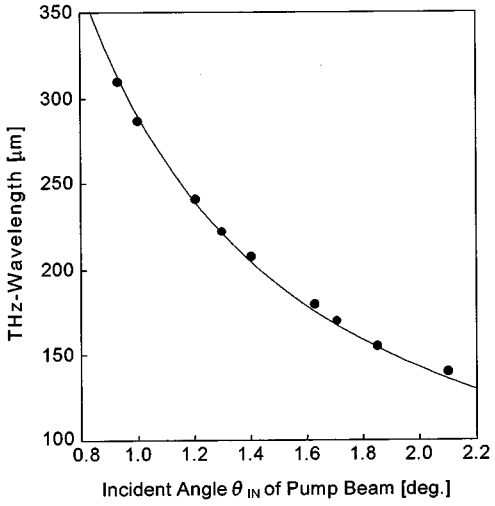

Fig. 4. Tuning characteristics of the terahertz wave using $LiNbO_3$ crystal. The solid curve indicates the values calculated from the noncollinear phase-matching condition.

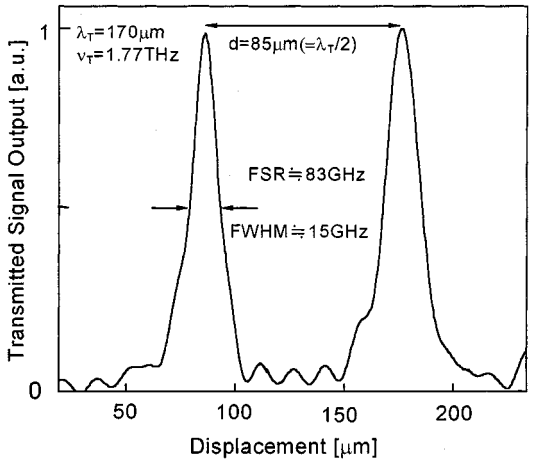

Fig. 5. Example of spectral measurements of the terahertz wave using a metal mesh F–P interferometer. The distance between the peaks corresponds to the half-wavelength of the terahertz wave.

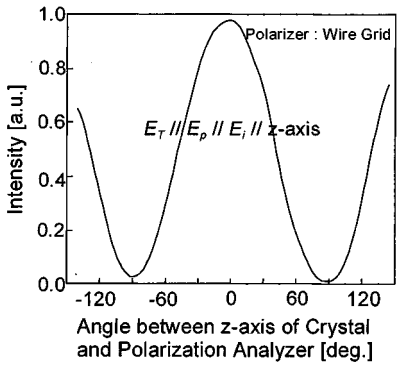

Fig. 6. Measured polarization of the generated terahertz wave using a wire grid polarizer. The linear polarization characteristics originates from the stimulated parametric interaction process.

III. Experiments

A. Experimental Setup

A schematic diagram of the experimental setup is shown in Fig. 2. The pump source was a Q-switched Nd : YAG laser (Solar LF113, wavelength: 1.064 μm, pulsewidth: 25 ns) whose polarization was along the z-axis of $LiNbO_3$. A 5-mm-thick $LiNbO_3$ z-plate that was 65-mm long along the x-axis was cut. The ends of the plate were cut parallel in the x-plane, polished and antireflection (AR) coated for operation at wavelengths around 1.07 μm. A prism (bottom angle $\cong$39°) made of high-resistivity Si ($\rho > 1000$ Ωcm, $\alpha \cong 0.6$ cm^{-1}) was pressed against the y-surface of the crystal with an adjustable spring. High-reflection (HR)-coated mirrors M1 and M2 form an external resonator for the near-infrared idler wave. The cavity length was 15 cm, and the whole system, including the pump source, fits on a tabletop. The terahertz-wave output was detected using a 4K Si bolometer or a Schottky barrier diode, and its wavelength was measured with a metal mesh Fabry–Perot (F–P) interferometer [35] using an Ni mesh with a 65-μm grid.

B. Characteristics of $LiNbO_3$ TPO

Changing the incidence angle θ_{IN} of the pump beam from 1° to 2°, changed the phase-matching angles θ (between the pump and the idler) and δ (between the idler and the terahertz wave) from approximately 0.5° to 1° and 65° to 66°, respectively. The corresponding wavelengths of the idler and terahertz waves can be tuned from 1.068 to 1.072 μm and 290 to 150 μm, respectively. The angle-tuning characteristics agreed well with the value calculated from literature data [25], [36], as shown in Fig. 4. The signal output from the Si prism coupler was measured to be more than 0.1 nJ/pulse (peak power: 10 mW, pulsewidth: 10 ns) with a pump input of 30 mJ/pulse, where the typical oscillation threshold was around 20 mJ/pulse. An example of the spectral measurement of a terahertz wave is shown in Fig. 5. The free spectral range (FSR) of the F-P interferometer was about 83 GHz, and the linewidth was measured to be less than 15 GHz. A much narrower linewidth can obtained by introducing a spectral narrowing element, such as a grating or etalon, using an injection seeding method, or using a quasi-phase-matching method using periodically poled $LiNbO_3$ [37], [38]. Fig. 6 shows the polarization characteristics determined using a wire grid polarizer, and the terahertz wave is linearly polarized along the z-axis of the crystal. The observed terahertz-wave beam had an approximately Gaussian profile with a 5-mm beam radius (defined by the e^{-2} power) at a distance of 50 cm from the prism. The beam divergence was less than 0.7°.

We also investigated the cryogenic characteristics of the terahertz output [21], [22] from the $LiNbO_3$ TPO. The $LiNbO_3$ crystal was placed in a compact cryostat that could cool the crystal to the temperature of liquid nitrogen. The cryostat has AR-coated BK7 windows for the pump and idler waves, and a TPX (4-methyl penten-1) window for the terahertz wave. When the crystal was cooled to 78K, the terahertz-wave output was enhanced 125 times and the oscillation threshold decreased by 32% when operating at wavelengths around 180 μm. The contributions of the enhanced parametric conversion efficiency and

the reduced absorption loss of the terahertz wave during the propagation inside the $LiNbO_3$ crystal were found to be comparable. As described in parametric gain theory (Section II-B), the mechanism is explained by the reduction of the linewidth of the lowest A_1-symmetry phonon mode.

C. Characteristics of the MgO : LiNbO$_3$ TPO

1) Parametric Generation Characteristics: We further studied other nonlinear materials, such as $LiTaO_3$ and $MgO:LiNbO_3$, that have a much larger photorefractive resistance than that of undoped $LiNbO_3$. $MgO:LiNbO_3$ crystal is remarkably more resistant to optical damage than an undoped crystal [27], and very efficient nonlinear frequency conversion (second harmonic generation [28], optical parametric oscillator [29]) was reported in the visible and near infrared region. To study the performance in our terahertz regime, we initially measured the single-pass parametric generation (terahertz-wave parametric generation: TPG) characteristics, where the angle dependence of the idler wavelength determines the dispersion relationships of the lowest A_1-symmetry polariton mode or angle-tuning characteristics of the TPO, and the broad-band TPG output shows the gain profile or tuning range of idler and terahertz waves. 5-mm-thick-undoped (congruent) and 5-mol% MgO-doped $LiNbO_3$ crystals were cut into pieces 65-mm long along the x-axis, and their end surfaces were AR coated for operation at around 1.07 μm. The pump source was a Q-switched Nd : YAG laser (New Wave Research MiniLase II, wavelength: 1.064 μm, pulsewidth: 7 ns), the typical output was 10 mJ/pulse, and the polarization was along the z-axis of the samples. The idler (or TPG) outputs and the spectra were measured with an optical spectrum analyzer.

Fig. 7 shows the dispersion relationships of the polariton and the TPG output characteristics. The measured dispersion curves were almost the same; thus, there are no significant differences in the angle-tuning characteristics of the undoped and MgO-doped samples. However, the idler intensity (TPG output) was enhanced nearly threefold and the peak shifted to the higher energy side with the MgO-doped sample. The dope-level dependence of the TPG was also studied using 0-mol%-9-mol% $MgO:LiNbO_3$ samples. The maximum TPG output as well as the extension of tunability to the high-energy side of terahertz wave was obtained at 5 mol%, therefore, optimum dope level was found to be 5 mol%.

2) Measuring Raman Spectra: To study the enhancement mechanism in the MgO-doped sample, further microscopic information is required. Raman spectroscopy is one of the most effective methods because the Raman intensity (i.e., scattering cross section) is directly related to the parametric gain through the nonlinear coefficient d_Q (2), (4)–(6). In addition, the eigenfrequencies and linewidths of the A_1-symmetry phonon modes provide information on the absorption coefficient at terahertz frequencies. To study the A_1-symmetry mode, measurement was performed in the X(ZZ)Y configuration. The laser source was an argon ion laser (wavelength: 488 nm, power: 29 mW) and the Stokes photon was detected with a photomultiplier through a monochromator. The samples were the same as those used in the TPG experiment. The measurement was performed

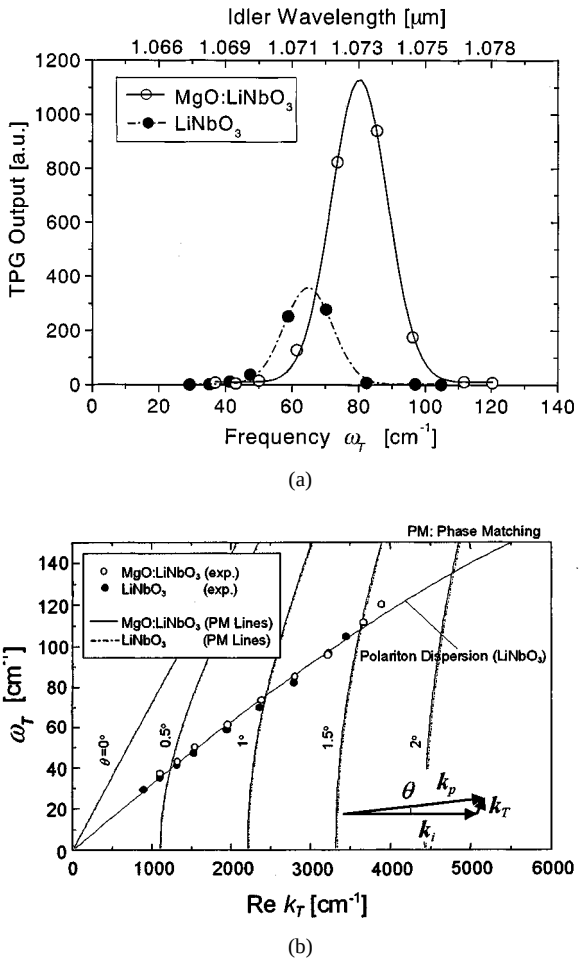

Fig. 7. TPG characteristics of undoped and 5-mol% MgO-doped $LiNbO_3$ pumped by a Q-swithed Nd : YAG laser. (a) Intensity of the generated idler or terahertz wave. (b) Dispersion relation of the A_1-symmetry polariton mode of these samples, which determines the angle-tuning characteristics of the TPO's.

from 50 to 450 cm^{-1} because the lowest mode is dominant in our terahertz regime.

Fig. 8 shows the increased Raman intensity of the lowest A_1 mode in the $MgO:LiNbO_3$, which is about 1.4 times larger than in the undoped sample. Thus, the enhancement of the TPG output or the parametric gain (5) was found to originate from the enhanced scattering cross section when the vacancy of the Li^+ site in the crystal is filled with Mg^{2+}. In addition, the eigenfrequencies of these samples from the lowest level to the third were not significantly different, which shows that the peak shift observed in the TPG spectra has no relation to the shift in the eigenfrequencies. The result is also consistent with the TPG experiment, in which the polariton dispersions of these samples were nearly the same. The absorption coefficient calculated from the imaginary part of the polariton wave vector (7) is nearly proportional to the linewidth of the lowest mode in the low energy region ($<$100 cm^{-1}). Therefore, the coefficient of the $MgO:LiNbO_3$ is slightly lower ($\sim$1.1 times) than that of the undoped $LiNbO_3$ (see Fig. 9).

It should be noted that the above results are somewhat different from those reported [39], [40] where measured eigenfrequencies of the A_1 modes were similar to ours, but $MgO:LiNbO_3$ exhibited broader linewidths and weaker

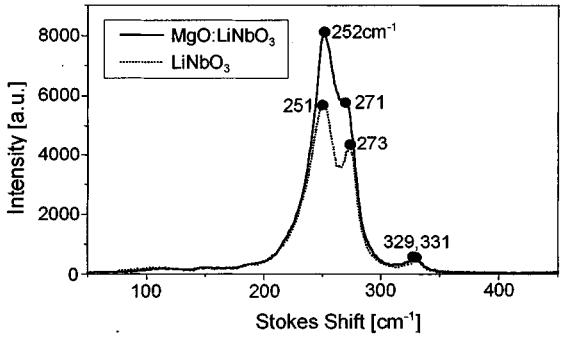

Fig. 8. Spontaneous Raman spectra of the A_1-symmetry phonon mode in undoped (congruent) $LiNbO_3$ (dotted line) and 5-mol% $MgO:LiNbO_3$ (solid line) at room temperature. The measurement was performed with the accuracy of absolute frequency of 0.3 cm^{-1}, and the resolution of less than 1 cm^{-1}. The spectral deconvolution study finds that the linewidths of the A_1-symmetry modes from the lowest to the third are 29.5, 12.5, and 22.0 cm^{-1} for the undoped $LiNbO_3$, and 25.5, 17.0, and 29.0 cm^{-1} for the $MgO:LiNbO_3$.

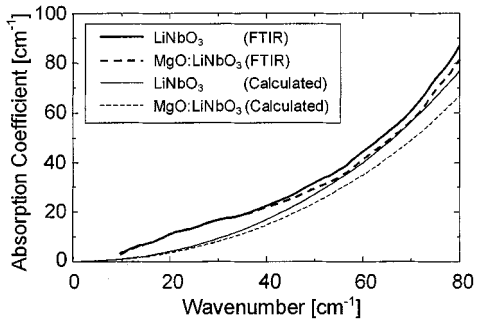

Fig. 9. Absorption coefficients of undoped and MgO-doped $LiNbO_3$ in the terahertz region at room temperature measured by the far-infrared transmittance (FTIR), and the values calculated from the complex polariton wave vector [see (7)] using the parameters determined by spontaneous Raman scattering.

Raman intensities. According to the analysis based on crystal imperfections [39]–[42], the quality of our $MgO:LiNbO_3$ crystal was better than those reported. In addition, consideration of the sum rule [43] lead us to further insights: Raman intensity, which reflects the sum of the number of states, is proportional to the optical conductivity. This implies that the conductivity is increased with the dope, whose picture is consistent to the reduction mechanism of photorefractive damages caused by the local charge generated [27]. The local current will also cause optical losses; thus, we infer that there must be a optimum MgO-doped level (we measured 5 mol%) to result in the maximum parametric gain. To obtain a complete understanding of the enhancement mechanism, a damping mechanism of the polariton should be studied in terms of not only the crystal imperfection, but also the charge–transfer mechanism. We are now preparing for Raman measurements with samples of different MgO concentrations to measure the linewidths as well as the scattering cross sections of the A_1 modes. Also, quantitative study on the parametric gain [41], [42] and examinations of samples with different dopants (e.g., ZnO, In_2O_5) or stoichiometric crystals are in progress.

3) Far-Infrared Transmittance: The far-infrared transmittance was also measured with a Fourier transformation infrared (FTIR) spectrometer with a 4K Si-bolometer detector. Samples with different thicknesses ($LiNbO_3$: 265 μm, 507 μm; 5-mol% $MgO:LiNbO_3$: 265 μm, 505 μm) were prepared to measure the absorption coefficient in the terahertz region. The measurement was performed at room temperature with a resolution of 4 cm^{-1}, and the results are shown in Fig. 9. The absorption loss of the terahertz wave inside the crystal was nearly the same in the undoped and MgO-doped samples. In Fig. 9, the reliability of the measured absorption coefficients was also checked using the values calculated from the imaginary part of the A_1-symmetry polariton wave vector (7) using the Raman data shown above (i.e., the eigenfrequencies and linewidths), and a good agreement is seen. In view of the TPG results, $MgO:LiNbO_3$ has much better properties than undoped $LiNbO_3$.

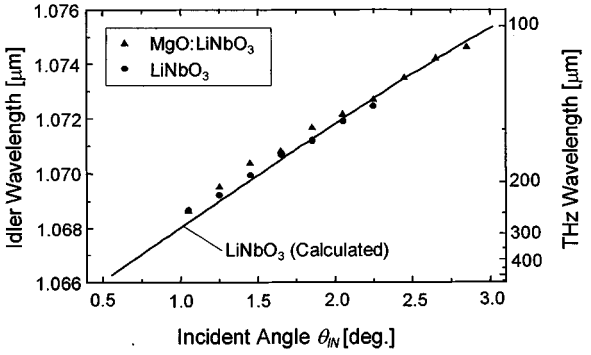

Fig. 10. Angle-tuning characteristics of terahertz wave for $LiNbO_3$ and $MgO:LiNbO_3$. The solid line shows the values calculated from the phase-matching condition for $LiNbO_3$.

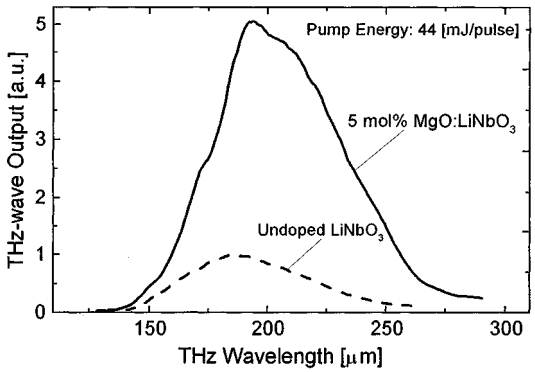

Fig. 11. Measured output characteristics of terahertz wave from $LiNbO_3$ and $MgO:LiNbO_3$ TPO's pumped at a fixed energy (44 mJ/pulse).

4) Characteristics of the $MgO:LiNbO_3$ TPO: The performances of the $MgO:LiNbO_3$ TPO were examined using the experimental setup shown in Fig. 2. The crystals were the same as those used in the TPG experiments, and they were mounted on a sliding stage to compare the TPO characteristics under the same conditions. The pump source was a Q-switched Nd:YAG laser (Lotis TII LS-2135-LP, $\lambda = 1.064$ μm, pulsewidth: 25 ns) polarized along the z-axis of the crystal, and a 4K Si-bolometer was used to detect the terahertz wave. As shown in Fig. 10, the angle-tuning characteristics of the TPO's using undoped and MgO-doped $LiNbO_3$ were nearly the same as those seen in the TPG experiment (Fig. 7). Due to the enhanced parametric gain (Fig. 7) and the similar loss properties of the terahertz wave (Fig. 9), however, the terahertz-wave output of $MgO:LiNbO_3$ TPO was nearly five times greater, as shown in Fig. 11.

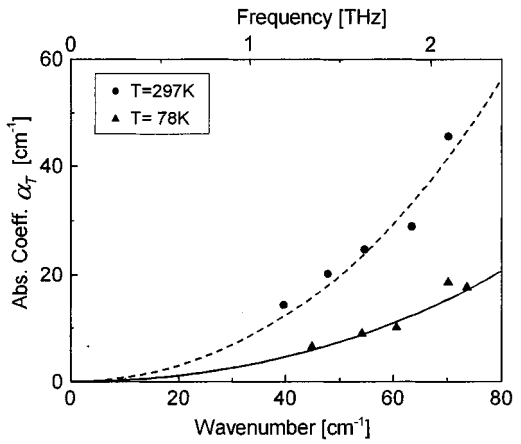

Fig. 12. Measured absorption coefficients of $LiNbO_3$ in the 1–2-THz region using the tunable terahertz-wave source of the TPO.

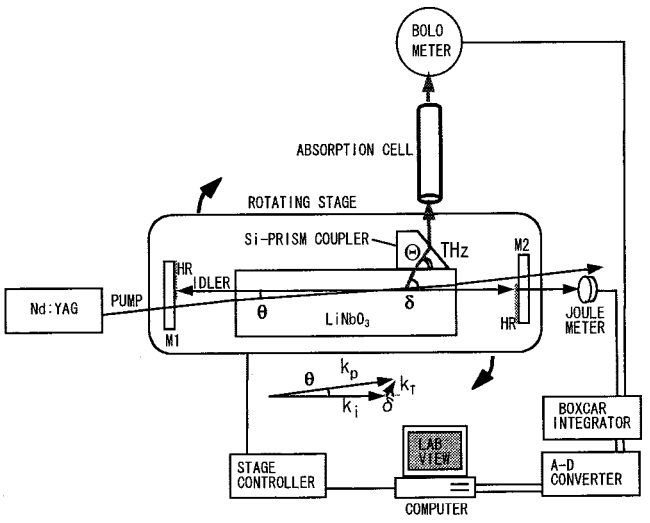

Fig. 13. Schematic diagram of the compact terahertz-wave spectrometer system using a TPO with an Si-prism coupler. By controlling the rotating stage, terahertz spectroscopy for a gas is easily achieved over the wide wavelength range.

IV. Application to Spectroscopy

A. Absorption Coefficient of $LiNbO_3$ in the Terahertz Region

A variety of applications are possible using this coherent tunable terahertz-wave source. First, we measured the absorption coefficient α_T of $LiNbO_3$ at terahertz frequency using this TPO as a coherent tunable source of terahertz waves. The $LiNbO_3$ crystal inside the cryostat was placed on a horizontally sliding stage so that the y-axis of the crystal was aligned with the direction of movement. The propagating length inside the $LiNbO_3$ crystal changes with the position of the crystal so that the absorption coefficient α_T can be obtained precisely by measuring the y-dependence of the terahertz-wave power [21]. Fig. 12 shows the measured α_T in the 1–2-THz region at room temperature and at the temperature of liquid nitrogen. The solid line indicates the values calculated from the complex polariton wave vectors. The results obtained are in good agreement with the calculated values from the polariton wave vectors [see (7)].

B. Terahertz Spectroscopy of Water Vapor

The absorption spectrum of water vapor in the air was also measured by constructing the terahertz-wave spectrometer shown in Fig. 13, where the terahertz-wave output from the prism was coupled into a 1-m-long metal hollow tube containing 1-atm air [19], [20]. The output was measured as a function of the incident angle of the pump beam to the crystal, and the background measurements were calibrated. The result is shown in Fig. 14. The spectral resolution is wider than the pressure-broadened water-absorption linewidth, thus, further spectral narrowing is necessary. We are already considering improving the cavity configuration using a grating or etalon, the injection-seeding method, or the quasi-phase-matching scheme, as mentioned above.

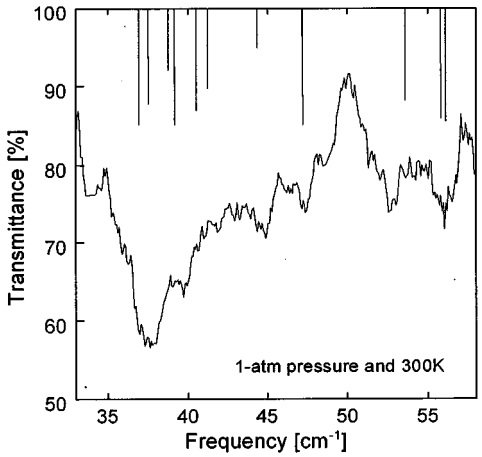

Fig. 14. Example of atmospheric transmission spectrum obtained by using the TPO-spectrometer terahertz wave passed through a 1-m-long absorption cell, which was filled with 1-atm air.

V. Conclusion

In this paper, we produced an efficient tunable TPO using $LiNbO_3$ and $MgO:LiNbO_3$ crystals. We measured the tunability, power, coherency, polarization, and beam divergence of this TPO, and demonstrated its use in terahertz spectroscopy. Our parametric method has significant advantages over other available sources of terahertz waves; i.e., it is compact, easy to use, and has a wide tunability. This method has many potential applications, including spectroscopic measurements of various materials, medical and biological applications, terahertz imaging, monitoring different gasses, use in communication, etc. Further study is required to increase its efficiency, narrow the linewidth, and establish a continuous-wave operation, possibly by utilizing a domain-inverted structure.

Acknowledgment

The authors are greatly indebted to the Yamaju Ceramics Company, Seto, Japan, for supplying the $MgO:LiNbO_3$ samples, and C. Takyu and T. Shoji for their excellent work coating and polishing of the crystals and mirrors. The authors would also like to thank Prof. Ushioda and Dr. Sakamoto, Tohoku University, Sendai, Japan, for measuring the Raman scattering.

REFERENCES

[1] P. R. Smith, D. H. Auston, and M. C. Nuss, "Subpicosecond photoconducting dipole antennas," *IEEE J. Quantum Electron.*, vol. 24, pp. 255–260, Feb. 1988.

[2] M. van Exter and D. Grischkowsky, "Characterization of an optpelectronic terahertz beam systems," *IEEE Trans. Microwave Theory Tech.*, vol. 38, pp. 1684–1691, Nov. 1990.

[3] M. C. Nuss and J. Orenstein, "Terahertz time-domain spectroscopy (THz-TDS)," in *Millimeter-Wave Spectroscopy of Solids*, G. Gruener, Ed. Berlin, Germany: Springer-Verlag, 1997.

[4] D. M. Mittleman, R. H. Jacobsen, and M. C. Nuss, "T-ray imaging," *IEEE J. Select. Topics Quantum Electron.*, vol. 2, pp. 679–691, Sept. 1996.

[5] P. Y. Han and X.-C. Zhang, "Coherent, broadband midinfrared terahertz beam sensors," *Appl. Phys. Lett.*, vol. 73, pp. 3049–3051, 1998.

[6] M. Tani, R. Fukasawa, H. Abe, S. Matsuura, K. Sakai, and S. Nakashima, "Terahertz radiation from coherent phonons excited in semiconductors," *J. Appl. Phys.*, vol. 83, pp. 2473–2477, 1998.

[7] N. Sarukura, H. Ohtake, S. Izumida, and Z. Liu, "High average-power THz radiation from femtosecond laser-irradiated InAs in a magnetic field and its elliptical polarization characteristics," *J. Appl. Phys.*, vol. 84, pp. 654–656, 1998.

[8] M. Hangyo, S. Tomozawa, Y. Murakami, M. Tonouchi, M. Tani, Z. Wang, K. Sakai, and S. Nakashima, "Terahertz radiation from superconducting $YBa_2Cu_3O_{7-\delta}$ thin films excited by femtosecond optical pulses," *Appl. Phys. Lett.*, vol. 69, pp. 2122–2124, 1996.

[9] S. Zernike, Jr. and P. R. Berman, "Generation of far infrared as a difference frequency," *Phys. Rev. Lett.*, vol. 15, pp. 999–1001, 1965.

[10] R. Morris and Y. R. Shen, "Theory of far-infrared generation by optical mixing," *Phys. Rev. A, Gen. Phys.*, vol. 15, pp. 1143–1156, 1977.

[11] E. B. Brown, K. A. McIntosh, K. B. Nichols, and C. L. Dennis, "Photomixing up to 3.8 THz in low temperature-grown GaAs," *Appl. Phys. Lett.*, vol. 66, pp. 285–287, 1995.

[12] S. Matsuura, M. Tani, H. Abe, K. Sakai, H. Ozeki, and S. Saito, "High-resolution terahertz spectroscopy by a compact radiation source based on photomixing with diode lasers in a photoconductive antenna," *J. Mol. Spectrosc.*, vol. 187, pp. 97–101, 1998.

[13] J. M. Yarborough, S. S. Sussman, H. E. Puthoff, R. H. Pantell, and B. C. Johnson, "Efficient tunable optical emission from $LiNbO_3$ without a resonator," *Appl. Phys. Lett.*, vol. 15, pp. 102–105, 1969.

[14] M. A. Piestrup, R. N. Fleming, and R. H. Pantell, "Continuously tunable submillimeter wave source," *Appl. Phys. Lett.*, vol. 26, pp. 418–421, 1975.

[15] K. Kawase, M. Sato, T. Taniuchi, and H. Ito, "Coherent tunable THz-wave generation from $LiNbO_3$ with monolithic grating coupler," *Appl. Phys. Lett.*, vol. 68, pp. 2483–2485, 1996.

[16] ——, "Characteristics of THz-wave radiation using a monolithic grating coupler on a $LiNbO_3$ crystal," *Int. J. Infrared Millim. Waves*, vol. 17, pp. 1839–1849, 1996.

[17] K. Kawase, M. Sato, K. Nakamura, T. Taniuchi, and H. Ito, "Unidirectional radiation of widely tunable THz-wave using a prism coupler under noncollinear phase matching condition," *Appl. Phys. Lett.*, vol. 71, pp. 753–755, 1997.

[18] T. Walther, K. R. Chapin, and J. W. Beven, "Comment on 'Unidirectional radiation of widely tunable THz-wave using a prism coupler under noncollinear phase matching condition'," *Appl. Phys. Lett.*, vol. 73, pp. 3610–3611, 1998.

[19] H. Ito, K. Kawase, and J. Shikata, "Widely tunable THz- wave generation by nonlinear optics," *IEICE Trans. Electron.*, vol. E81-C, pp. 264–268, 1998.

[20] K. Kawase, J. Shikata, M. Sato, T. Taniuchi, and H. Ito, "Widely tunable coherent THz-wave generation using nonlinear optical effect," *Electron. Commun. Japan*, pt. 2, vol. 7, pp. 10–18, 1998.

[21] J. Shikata, K. Kawase, M. Sato, T. Taniuchi, and H. Ito, "Enhancement of terahertz-wave output from $LiNbO_3$ optical parametric oscillators by cryogenic cooling," *Opt. Lett.*, vol. 24, pp. 202–204, 1999.

[22] ——, "Characteristics of coherent terahertz wave generation from $LiNbO_3$ optical parametric oscillator," *Electron. Commun. Japan*, pt. 2, vol. 82, pp. 46–53, 1999.

[23] D. N. Nikogosyan, "$LiNbO_3$, Lithium Niobate," in *Handbook of Nonlinear Optical Crystals*, V. G. Dmitriev, G. G. Gurzadyan, and D. N. Nikogosyan, Eds. Berlin, Germany: Springer-Verlag, 1997.

[24] I. Shoji, T. Kondo, A. Kitamoto, M. Shirane, and R. Ito, "Absolute scale of second-order nonlinear-optical coefficients," *J. Opt. Soc. Amer. B, Opt. Phys.*, vol. 14, pp. 2268–2294, 1997.

[25] E. D. Palik, "Lithium Niobate ($LiNbO_3$)," in *Handbook of Optical Constants of Solids*, E. D. Palik, Ed. New York: Academic, 1985.

[26] D. F. Edwards, "Sillicon (Si)," in *Handbook of Optical Constants of Solids*, E. D. Palik, Ed. New York: Academic Press, 1985.

[27] Y. Furukawa, M. Sato, F. Nitanda, and K. Ito, "Growth and characterization of MgO-doped $LiNbO_3$ for electro-optic devices," *J. Cryst. Growth*, vol. 99, pp. 832–836, 1990.

[28] J. L. Nightingale, W. J. Silva, G. E. Reade, A. Rybicki, W. J. Kozlovsky, and R. L. Byer, "Fifty percent efficiency second harmonic generation in magnesium oxide doped lithium niobate," in *Proc. SPIE-Int. Soc. Opt. Eng.*, vol. 681, 1987, pp. 20–24.

[29] D. C. Gerstenberger and R. W. Wallance, "Continuous-wave operation of a doubly resonant lithium niobate optical parametric oscillator system tunable from 966–1185 nm," *J. Opt. Soc. Amer. B, Opt. Phys.*, vol. 10, pp. 1681–1683, 1993.

[30] Y. R. Shen, "Stimulated polariton scattering," in *The Principle of Nonlinear Optics*. New York: Wiley, 1984.

[31] H. E. Puthoff, "The stimulated Raman effect and its application as a tunable laser," Stanford Univ., Stanford, CA, Microwave Lab. Rep. 1547, 1967.

[32] S. S. Sussman, "Tunable light scattering from transverse optical modes in lithium niobate," Stanford Univ., Stanford, CA, Microwave Lab. Rep. 1851, 1970.

[33] W. D. Johnston Jr. and I. P. Kaminow, "Temperature dependence of Raman and Rayleigh scattering in $LiNbO_3$ and $LiTaO_3$," *Phys. Rev.*, vol. 158, pp. 1045–1054, 1968.

[34] A. Yariv, *Quantum Electronics*. New York: Wiley, 1989.

[35] K. Sakai, T. Fukui, Y. Tsunawaki, and H. Yoshinaga, "Metallic mesh bandpass filters and Fabry–Perot interferometer for the far infrared," *Jpn. J. Appl. Phys.*, vol. 8, pp. 1046–1055, 1969.

[36] G. J. Edwards and M. Lawrence, "A temperature-dependent dispersion equation for congruently grown lithium niobate," *Opt. Quantum Electron.*, vol. 16, pp. 373–375, 1984.

[37] K. Kawase and H. Ito, "Submillimeter generation using periodic domain reversal," *Nonlinear Opt.*, vol. 7, pp. 225–229, 1994.

[38] Y. J. Ding and J. B. Khurgin, "A new scheme for efficient generation of coherent and incoherent submillimeter to THz waves in periodically poled lithium niobate," *Opt. Commun.*, vol. 148, pp. 105–109, 1998.

[39] S. Kojima, "Composition variation of optical phonon damping in lithium niobate crystals," *Jpn. J. Appl. Phys.*, vol. 32, pp. 4373–4376, 1993.

[40] U. T. Schwartz and M. Maier, "Asymmetric Raman lines caused by an an harmonic lattice potential in lithium niobate," *Phys. Rev. B, Condens. Matter*, vol. 55, pp. 11041–11044, 1997.

[41] ——, "Frequency dependence of phonon polariton damping in lithium niobate," *Phys. Rev. B, Condens. Matter*, vol. 53, pp. 5074–5077, 1996.

[42] ——, "Damping mechanism of phonon polaritons, exploited by stimulated Raman gain measurements," *Phys. Rev. B, Condens. Matter*, vol. 58, pp. 766–775, 1998.

[43] A. S. Barker and R. Loudon, "Response functions in the theory of Raman scattering by vibrational and polariton modes in dielectric crystals," *Rev. Mod. Phys.*, vol. 44, pp. 18–47, 1972.

[44] Y.-R. Shen, "Infrared generation by stimulated Raman scattering," in *Nonlinear Infrared Generation*, Y.-R. Shen, Ed. Berlin, Germany: Springer-Verlag, 1977.

Jun-ichi Shikata was born in Kyoto, Japan, on June 29, 1969. He received the B.S., M.S., and Ph.D. degrees in electronic engineering from Tohoku University, Sendai, Japan, in 1992, 1994, and 1998, respectively.

Since 1998, he has been a Research Associate at Research Institute of Electrical Communication, Tohoku University, where, since 1996, he has been engaged in research on terahertz-wave generation using nonlinear optics.

Dr. Shikata is a member of the Japan Society of Applied Physics, the Optical Society of Japan (OSJ), the Physical Society of Japan, and the Optical Society of America (OSA).

Kodo Kawase was born in Kyoto, Japan, on September 14, 1966. He received the B.S. degree in electronic engineering from Kyoto University, Kyoto, Japan, in 1989, and the M.S. and Ph.D. degrees in electronic engineering from Tohoku University, Sendai, Japan, in 1992 and 1996, respectively.

From 1989 to 1990, he was with the Research Development Corporation of Japan (JRDC). In 1996, he became a COE Researcher at the Research Institute of Electrical Communication, Tohoku University, and a Research Associate and a Assistant Professor at Tohoku-Gakuin University in 1997 and 1998, respectively. He has been a COE Researcher at the Communications Research Laboratory (CRL) since 1995. He is currently with the Photo Dynamics Research Center, Institute of Physical and Chemical Research (RIKEN), Sendai, Japan, where, since 1992, he has been involved in research on terahertz-wave generation using nonlinear optics.

Dr. Kawase is a member of the Institute of Electronics, Information and Communication Engineers (IEICE), Japan, and the Japan Society of Applied Physics. He received the Encouragement Award presented by the Japan Society of Applied Physics, and the Best Paper Award presented the Laser Society of Japan.

Ken-ichi Karino was born in Yamagata, Japan, on June 12, 1975. He received the B.S. degree in electronic engineering from Tohoku University, Sendai, Japan, in 1998, and is currently working toward the M.S. degree.

Since 1997, he has been engaged in research on terahertz-wave generation using nonlinear optics.

Tetsuo Taniuchi was born in Chiba, Japan, on September 23, 1950. He received the B.S., M.S., and Ph.D. degrees in communication engineering from Tohoku University, Sendai, Japan, in 1973, 1975, and 1978, respectively.

In 1978, he joined the Central Research Laboratory, Matsushita Electric Industrial Corporation Ltd., Osaka, Japan. In 1993, he became an Associate Professor at the Institute of Material Research, Tohoku University. Since 1995, he has been an Associate Professor at the Research Institute of Electrical Communication, Tohoku University, where he currently is engaged in research on nonlinear optical devices and integrated photonics.

Dr. Taniuchi is a member of the Institute of Electronics, Information and Communication Engineers (IEICE), Japan, and the Japan Society of Applied Physics.

Hiromasa Ito (M'87–SM'98) was born in Tokyo, Japan, on August 31, 1943. He received the B.S. degree in communication engineering, and the M.S. and Ph.D. degrees in electronic engineering from Tohoku University, Sendai, Japan, in 1966, 1969, and 1971, respectively.

In 1972, he joined the Research Institute of Electrical Communication, Tohoku University, where he is currently a Professor, and the Head of the Applied Quantum Optics Research Division. From 1975 to 1976, while on leave from Tohoku University, he was with the Ginzton Laboratory, Stanford University, where he was involved in research on parametric oscillators. Since 1998, he has been a Team Leader of the "Tera-Photonics" project of the Photo Dynamics Research Center, RIKEN, Sendai, Japan. His research interests have included lasers, nonlinear optics (especially using periodically domain inverted structures), semiconductor lasers, and coherent terahertz-wave generation.

Dr. Ito is a member of the Institute of Electronics, Information and Communication Engineers (IEICE), Japan, the Japan Society of Applied Physics, the Optical Society of Japan (OSJ), the Laser Society of Japan, and the Optical Society of America (OSA). He received the 1971 Yonezawa Award and the 1989 Best Paper Award presented by the IEICE, Japan.